Journal of Inorganic and Organometallic Polymers and Materials, Vol. 16, No. 2, June 2006 (© 2006)
DOI: 10.1007/s10904-006-9037-8

A Study of Encapsulation Resin Containing Hexagonal Boron Nitride (hBN) as Inorganic Filler

Tzu Hsuan Chiang[1] and T.-E. Hsieh[1,2]

Preparation and property characterization of encapsulation resin contained hexagonal boron nitride (hBN) as inorganic filler were carried out in this work. The dielectric properties, coefficient of thermal expansion (CTE), thermal conductivity, curing kinetics, adhesion strength and viscosity of the resins with the load of hBN filler ranging from 9.2 to 25.7 vol.% (20–70 wt.%) were evaluated. It was found that the dielectric properties of resin containing SiO_2 filler are inferior to that containing hBN. Also, the resins possessed lower CTE and the higher T_g when the hBN contents were high (>15 vol.%) and the resin containing 25.7 vol.% hBN exhibited the largest thermal conductivity of 1.08 W/m K. Adhesion strength of the composite resins decreased with increase of hBN content and the adhesion strength on various substrates was found to be in the order of: alumina > Si wafer > eutectic PbSn solder.

KEY WORDS: encapsulation resin; hexagonal boron nitride (hBN); inorganic filler.

1. INTRODUCTION

The pursuit of high speed and high performance of electronic products raises the size and device density of IC chips. The power consumption increases accordingly and, for the development of encapsulation resins for IC chips, satisfactory heat dissipation ability is essential. Epoxide resin is one of the most popular organic materials for encapsulation resin due to its relatively low price, excellent processing ability and low viscosity. Its deficiencies include low thermal conductivity and high CTE and inorganic fillers such as silica [1–3], silicone carbide (SiC) [4, 5], alumina (Al_2O_3) [5, 6], aluminum nitride (AlN) [7–9] and boron nitride (BN)[10] have been added into the resin matrix to form the composite resin with satisfactory properties. However, the dielectric constants of SiC, Al_2O_3, AlN, etc. are relatively high, which are undesired for electronic packaging that always requires low dielectric properties.

Hexagonal boron nitride, hBN, has crystal structure similar to graphite (a = 0.25040, c = 0.66612) [11] except for the difference in the stacking of layers. hBN is a naturally lubricious material in its powder form and is often called white graphite. It is also an electrical insulator and exhibits excellent resistance to oxidation, performs exceptionally well at high temperatures (up to 3000°C), and is resistant to corrosive attack. Most of the applications of hBN are thermal dissipation, lubricant, hot-pressed shapes and pyrolytic shapes [12]. However, few studies were related to the epoxy resins containing hBN. The purpose of this work is hence to investigate the key properties including dielectric properties, CTE, thermal conductivity, adhesion strength, curing kinetics and viscosity of epoxied resins containing various amounts of hBN so as to explore the feasibility of hBN as the inorganic filler of encapsulation resins for device packaging.

[1] Department of Materials Science and Engineering, National Chiao Tung University, 1001 Ta-Hsueh Road, Hsinchu, 30050, Taiwan ROC.
[2] To whom correspondence should be addressed.
E-mail: tehsieh@cc.nctu.edu.tw

1574-1443/06/0600-0175/0 © 2006 Springer Science+Business Media, Inc.

2. EXPERIMENTAL

2.1. Materials and Sample Preparation

3,4-epoxy cyclohexylmethyl-3, 4-epoxy, hexahydro-4-methylphthalic anhydride was supplied by Adrich. The molecular weight and epoxy equivalent weight (EEW) of the epoxide resin is 252.3 g/mol and 133 g, respectively. The hardener is hexahydro-4-methylphthalic anhydride (HMPA) purchased from Aldrich and was used as received. The HMPA molecular weight is 168.2 g/mol and its purity is better than 97%. The ratio of epoxy to hardener was 1:1 based on the EEW and the hardener. About 0.5 wt.% of 2,4,6-tris(dimethylaminomethyl)phenol from TCI was used as the curing catalyst and 1 wt.% of γ-glycidoxypropyltrimethoxysilane from Aldrich was used as the coupling agent. The hBN filler supplied by National Nitride Technologies Co., Taiwan, possesses average particle sizes = 2–4 μm, density = 2.1 g/cm^3, tap density = 0.35 g/cm^3, dielectric constant = 4, and CTE = 1 ppm/°C. The SiO_2 filler supplied by Japanese High Purity Chemicals is quartz base with average particle sizes = 4 μm, density = 2.65 g/cm^3, dielectric constant = 3.8–4, and CTE = 12.3 ppm/°C.

The composite resin was prepared by first stirring the mixture of epoxide resin, hardener, curing catalyst and coupling agent for 2 h. The hBN filler was added into the organic mixture via a milling process using a triple rollers mill (EXAKT, Germany). SiO_2 filler was added into the organic mixture in a stepwise manner and then stirred for 2 h. The curing of all composite resin samples was carried out at 150°C for 1 h. In below, the composite resins containing hBN and SiO_2 fillers are termed as the hBN-resins and SiO_2-resins, respectively.

2.2. Property Characterizations

2.2.1. Dielectric Properties

Dielectric constants (ε) and tangent loss (tan δ) of composite resins were measured by a Hewllet Packard 4291B impedance analyzer incorporating with a HP 16453A test fixture at the frequencies ranging from 1 MHz to 1.0 GHz [12]. The disc-like sample, about 3 mm in thickness and 15 mm in diameter, was inserted in between the electrodes and the measurement was carried out in accord with ASTM D150 test standard. The dielectric properties of the sample were calculated via the equations as follows:

$$\varepsilon = \frac{\dot{Y}_{\mathrm{m}}}{j_{\omega} C_0 (1 + E_{\mathrm{edge}})}, \tag{1}$$

$$\tan \delta = D. \tag{2}$$

In above, $\dot{Y}_{\mathrm{m}}$ = measured admittance of sample, C_0 = the capacitance of parallel electrodes with spacing equal to sample thickness, $\omega = 2\pi f$ = angular frequency where f is the measured frequency in Hz, $E_{\mathrm{edge}} = 434 t^{0.825} \varepsilon^{-0.554}$ = the compensation coefficient resulted from the edge effect of HP 16453A test fixture (t = sample thickness), and D = dissipation factor.

2.2.2. Curing Kinetics of Resins

A differential scanning calorimeter (DSC, TA 2970) operating at a heating rate of 100°C/min was utilized to analyze the curing kinetics of resin samples. Samples containing 9.2, 11.2, 13.1, 15.0, 20.0, and 25.7 vol.% hBN filler were individually sealed in DSC pan then the isothermal scan at 150°C was performed in an ambient purged with nitrogen gas (50 cc/min). The extent of the reaction, or the conversion as a function of time, could be determined by integrating the isothermal curves using the following relationship [13]

$$\mathrm{Conversion}(\%) = \frac{100}{\Delta H_{\mathrm{T}}} \int_0^t \frac{dH}{dt} dt \tag{3}$$

where ΔH_{T} is total enthalpy change calculated from the integration of dH/dt from $t = 0$ to $t = \infty$.

The glass transition temperatures (T_g) of the samples were also determined by DSC. The samples were heated in the DSC cell with a heating rate of 5°C/min by around 250°C to obtain the curing profiles and the transition points of the profile were adopted as the T_g's of composite resins.

2.2.3. Coefficient of Thermal Expansion

The CTE's of the samples were measured by a thermomechanical analyzer (TMA, TA 2940). The cured sample was then cut by a diamond saw into square shape with dimensions approximately equal to 5 mm × 5 mm × 3 mm. Heat was applied from room temperature to around 250°C at a heating rate of 5°C/min after the sample was placed in the TMA cell. The CTE was calculated according to the plot of thermal expansion vs. temperature.

2.2.4. Thermal Conductivity

Thermal conductivity (κ) of the samples was measured by using an apparatus established by Microelectromechanical Systems of Electronics Research and Service Organization of Industrial Technology Research Institute (ERSO/ITRI) at Taiwan. The test assembly is schematically drawn in Fig. 1 [14]. The resin sample in a form of 30 mm × 30 mm × 6 mm was inserted in between two copper (Cu) blocks separately maintained at low (initially at 80°C) and high temperatures. During measurement, the energy transfer rate at the low-temperature Cu block, $\Delta Q/\Delta t$, was calculated according to

$$\frac{\Delta Q}{\Delta t} = \rho C_P V \frac{dT}{dt} \tag{4}$$

where ρ, C_P, and V are density, specific heat and volume of Cu block, and dT/dt is the heating rate of low-temperature Cu block that could be obtained from the slope of temperature change vs. time plot. Fourier's law can be expressed as

$$\frac{\Delta Q}{\Delta t} = \kappa A \frac{\Delta T}{\Delta x} \tag{5}$$

where A and Δx are the cross-sectional area for heat transfer and thickness of the sample under test, and ΔT is the temperature differential between two Cu blocks. The thermal conductivity of tested sample was calculated according to the equation derived from the equality of Eqs. (4) and (5)

$$\kappa = \frac{\rho C_P V \Delta x}{A \Delta T} \cdot \frac{dT}{dt} \tag{6}$$

2.2.5. Morphology

Morphologies of composite resins containing hBN and SiO_2 fillers were examined by a scanning electron microscope (SEM, Hitachi S-4700).

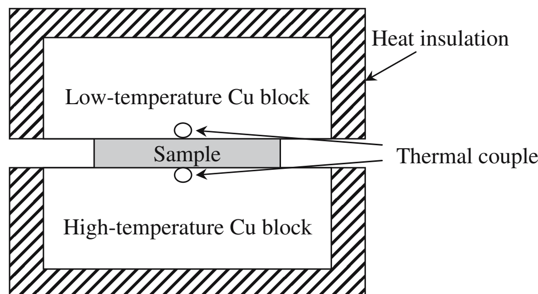

Fig. 1. Test assembly of thermal conductivity measurement.

2.2.6. Adhesion Strength

Adhesion strengths of resin samples were measured according to ASTM D897 test standard. The glass block was first polished into a truncated shape with top surface area equal to 5 mm × 10 mm. After applying the resin sample onto this area, the glass block was glued to various types of substrate materials including Al_2O_3, eutectic PbSn solder, Si wafer, and epoxy-based printed circuit board (PCB) to form the pull test specimens. Two steel bars were then attached to the two ends of the pull test samples and transferred to a pull tester (HT-8116, Hung Ta Instrument Co., Taiwan) operating at a pull rate of 5 mm/min for adhesion strength measurement.

2.2.7. Viscosity Measurement

The viscosities of the hBN-resin were measured by a viscometer (BROOKFIELD RVDV-III+, USA) using #6 spindle at the rotating speed of 5 rpm at room temperature.

3. RESULTS AND DISCUSSION

3.1. The Types of Fillers on Dielectric Properties of Resins

Figure 2 shows that the dielectric constants of all resin samples decrease with the increase of test frequencies, which is normally observed in polar resins containing functional groups. Anhydride acid curing agent was commonly added in the underfill resin to

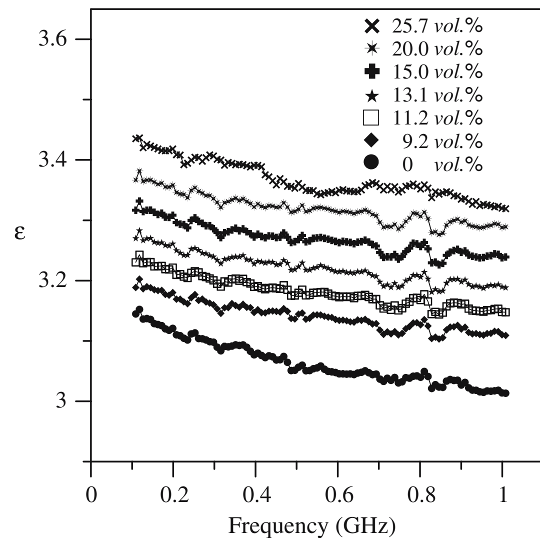

Fig. 2. Dielectric constants of hBN-resins as a function of test frequency.

reduce the viscosity. However, the hydroxyl (–OH) group forms in the anhydride-cured epoxy resins after the opening of an epoxide ring in further reactions [15]. Though epoxy resins have no specific molecular unit to raise the dielectric constant before curing, secondary alcoholic hydroxyl groups might generate after curing. The hydroxyl groups have an adverse effect on dielectric characteristics and raise the moisture absorption in the cured resins. Frommer *et al*. [16] reported that the dielectric constants of non-polar materials, such as PFTE, are nearly constant over a wide range of test frequencies. In contrast, for polar materials, such as phenolic resins or plasticized PVC, the dielectric constant decreases with the increase of frequency and most of thermoset resins tend to exhibit high dielectric constants due to their polar functionality.

Figure 2 also shows that the dielectric constants of composite resins increase with the increase of hBN content. The crystal structure of hBN is similar to that of graphite and mica that they both have molecularly smooth basal planes and no surface functional group is available for chemical bonding or interaction. However, at the edge planes of the hBN platelets, there are amine and hydroxyl groups available for chemical bonding [10]. Higher hBN filler content means more hydroxyl groups were incorporated and hence the increase of dielectric constant was observed [17].

Figure 3 shows the variation of dielectric constants of hBN- and SiO_2-resins measured at 1 GHz. Since the surface of SiO_2 filler contains more hydroxyl group, at the same filler loaded the dielectric constant of hBN-resin is thus lower than that of SiO_2-resin. This evidenced that the presence of polar groups in the filler and interfacial polarization indeed affects the dielectric properties of composite resins [18].

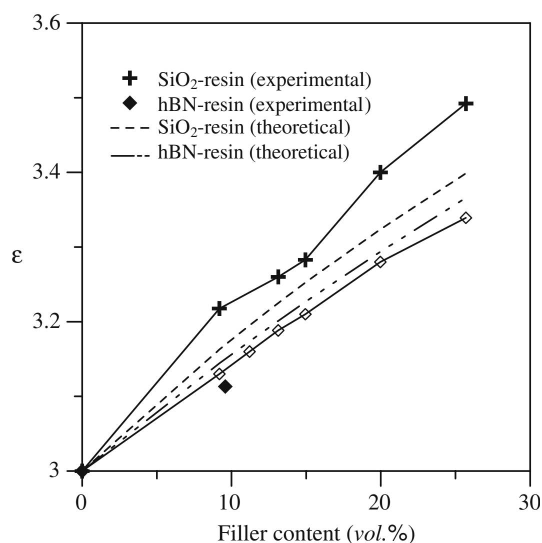

Fig. 3. Dielectric constants of composite resins as a function of filler content measured at 1 GHz.

The dielectric properties of composite material can be predicted according to following equations [17]:

$$\ln \varepsilon_c = \phi \ln \varepsilon_1 + (1 - \phi) \ln \varepsilon_2 \quad (7)$$

$$\ln(\tan \delta)_c = \phi \ln(\tan \delta)_1 + (1 - \phi) \ln(\tan \delta)_2 \quad (8)$$

where ε_c, ε_1, and ε_2 are the dielectric constants of the composite, filler, and resin matrix; $(\tan \delta)_c$, $(\tan \delta)_1$, and $(\tan \delta)_2$ are the tangent loss of the composite, filler, and resin matrix; ϕ is the volume fraction of filler. As shown in Fig. 3, dielectric constants obtained by theoretical calculation and experimental measurement show good coincidence for both types of composite resins. Furthermore, at the same filler loaded, the measured dielectric constants of hBN- and SiO_2-resins are lower than those obtained by computation. Such phenomenon was also observed in PTFE/SiO_2 composites system and was attributed to the non-uniform dispersion of inorganic filler in resin matrix [19].

Figure 4 shows the tangent loss as a function of filler content for the two composite resins measured at 1 GHz. At this testing frequency, the $\tan\delta$'s of SiO_2, hBN, and dicycloaliphatic epoxide are known to be 0.005 [16], 0.0003 [20], and 0.016 (measured value), respectively. Figure 4 shows that tangent loss property of hBN-resins is always better than that of SiO_2-resin. This should result from the lower $\tan\delta$ value and free of polar hydroxyl group on hBN filler

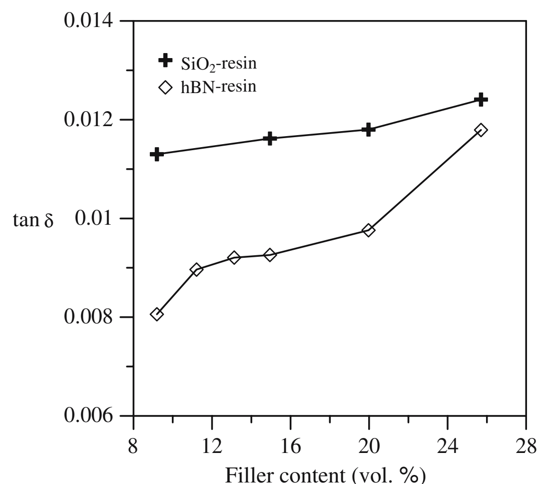

Fig. 4. Tangent loss of composite resins as a function of filler content measured at 1 GHz.

surface [20]. Figure 4 also shows that the $\tan\delta$'s of composite resins increase with the increase of filler content. Since $\tan\delta$ implies electrical energy dissipation during signal propagation, there hence exists a limitation on the inorganic filler content for underfill resins. Equation (8) predicts that addition of inorganic filler would suppress the tangent loss. However, as shown in Fig. 4, the tangent losses of hBN- and SiO_2-resins both increase with the increase of inorganic fillers. Such a phenomenon might result from the absorption of moisture on the surface of fillers. Since tangent loss of water is high as 35 [21], hence the tangent losses of composite resins increase with the amount of filler content.

3.2. Curing Kinetics

Based on the isothermal DSC characterizations, the heat flow of hBN-resins at 150°C as a function of time is plotted in Fig. 5. All curves in Fig. 5 show that a peak of initial reaction rate followed by a leveling down tail and the slope of profile becomes steeper when filler content is increased. The flat non-zero reaction rate tails reveal that there is a continuous curing reaction followed by the initial reaction. These tails evidence the existence of the diffusion-controlled reaction mechanism due to the increase of viscosity resulted from the peak reaction. The onset of the diffusion-controlled process indicates that fast transportation of the molecules in the resin system is prevented by the increase of viscosity [22].

The ΔH_T's of resins containing various amounts of filler were calculated based on the data of Fig. 5, which were then substituted into Eq. (3) to calculate the conversions of composite resins as shown in Fig. 6. Figures 5 and 6 show that when the hBN filler content is increased, the time to complete the curing of resin decreases and the conversion of resins increases. This evidences that the amine groups on the edge planes of hBN react with epoxy group of epoxide resin so as to accelerate the polymerization [23, 24]. Furthermore, increase of hBN filler content means more amine groups involve in the reactions with epoxide resin. This enhances the crosslinking, and therefore the T_g's of epoxide resins as listed in Table I.

Figure 7 depicts the isothermal DSC thermograms of hBN- and SiO_2-resins containing 25.7 vol.% filler. The shorter curing time of hBN-resin again evidences the existence of amine groups on hBN that promotes the polymerization of the epoxide resins.

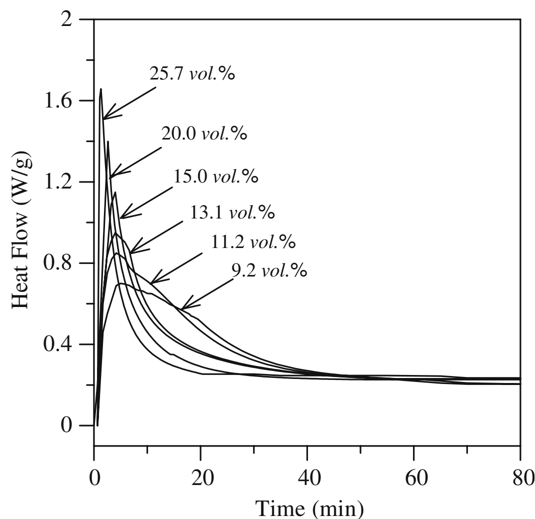

Fig. 5. Isothermal DSC thermograms of hBN-resins obtained at 150°C.

3.3. Coefficient of Thermal Expansion

Figure 8 shows the variation of CTE vs. the filler content of hBN-resin. It can be seen that the addition

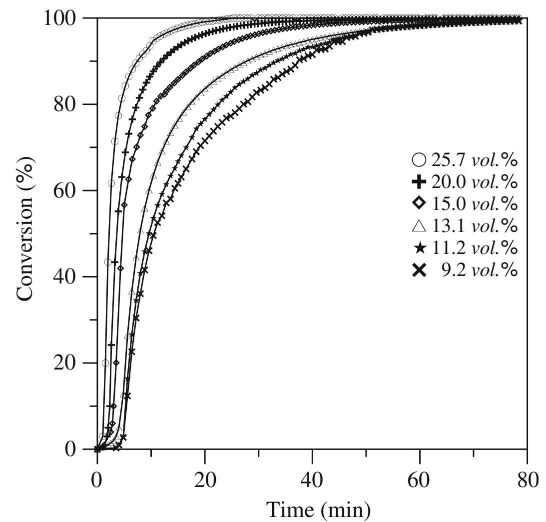

Fig. 6. Conversion of hBN-resins.

Table I. T_g of hBN-Resins Measured by DSC

hBN (vol.%)	T_g (°C)
25.7	148
20.0	130
15.0	125
13.1	123
11.2	120
9.2	118

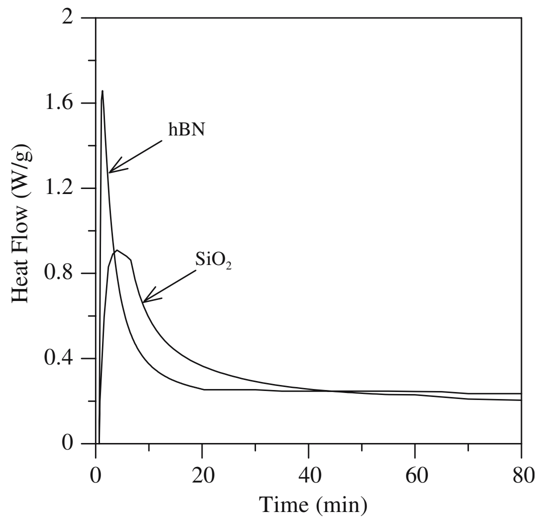

Fig. 7. Isothermal DSC thermograms of hBN and SiO_2-resins containing 25.7 vol.% filler.

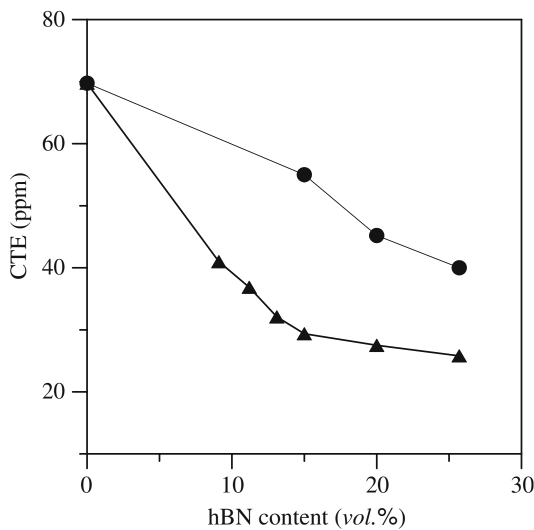

Fig. 8. CTE of various hBN content.

of inorganic filler effectively reduces CTE of organic resin, which evidences that the mechanical interlock at the organic–inorganic interface may constrain the CTE mismatch of the two components in composite resin. Figure 8 also shows that high hBN content (>15 vol.%) alleviates the reduction of CTE, which is similar to the behaviors SiO_2-resin reported peviously [25, 26]. According to our measurement, CTE of SiO_2-resin at 25.7 vol.% is 40 ppm, which is larger than 25.8 ppm for hBN-resin at the same filler content. This was attributed to the non-uniform dispersion of SiO_2 filler in resin matrix and quartz-SiO_2 filler possesses higher CTE.

3.4. Thermal Conductivity

Heat dissipation becomes an important issue in microelectronic packaging since the increase of device density drastically increases the electrical energy consumption. In comparison with metals and ceramics, polymers possess lower thermal conductivity due to relatively low atomic density. Nevertheless, such a deficiency could be improved by adding inorganic filler with high thermal conductivity in organic matrix.

Figure 9 shows the variation of thermal conductivity with the filler content for hBN- and SiO_2-resins. The thermal conductivities of both types of resins are enhanced with the increase of filler content, and the addition of hBN exhibits a better effect on the thermal conductivity enhancement. For hBN-resin containing 25.7 vol.% filler, the thermal conductivity reaches 1.08 W/m K [25], while for SiO_2-resin with the same filler content, the thermal conductivity is about 0.43 W/m K. This was attributed to the higher thermal conductivity property of hBN ($\kappa_{//}$ = 59 W/m K; $\kappa_{\perp} = 33$ W/m K) in comparison with that of SiO_2 filler (κ = 2–10 W/m K). Furthermore, the shape and dispersion of fillers in matrix might affect the thermal conductivity of composite resin. As shown in Fig. 10, the hBN-resin clearly exhibits a more uniform dispersion in resin matrix. It is noted that the surface area of filler increases with the increase of aspect ratio. The plate-like shape of hBN hence results a better inter-filler contact in comparison with the spherical filler at the same volume

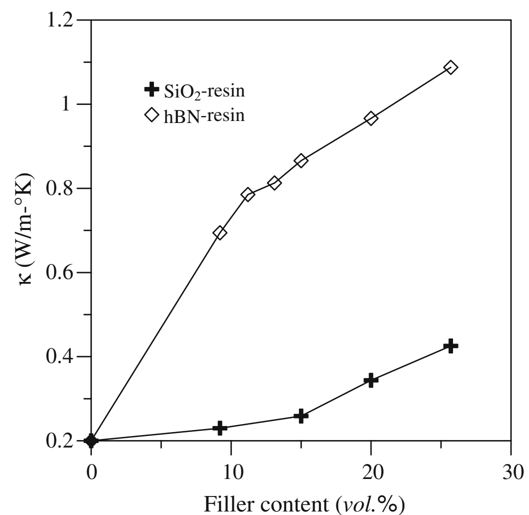

Fig. 9. Thermal conductivity of an EMC with various volume fractions of filler.

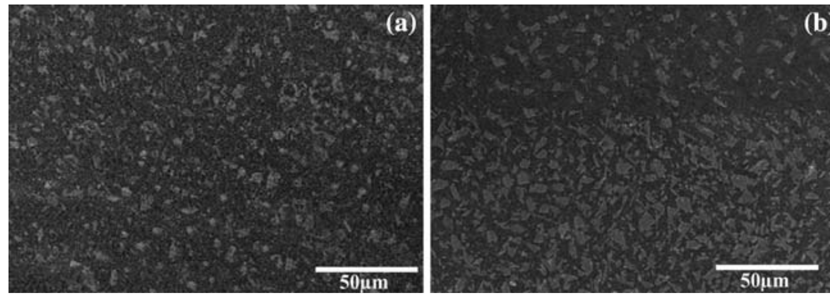

Fig. 10. SEM morphology of (a) hBN-resin and (b) SiO_2-resin (filler content = 25.7 vol.%).

loading [25] so that a better thermal conductivity property was observed in hBN-resin.

3.5. Adhesion Strength

Encapsulation resin might contact with IC chip, interconnect materials, assembly substrate, etc. [27, 28]. We hence measured the adhesion strengths of composite resins on Si wafer, eutectic PbSn solder, Al_2O_3, and PCB, respectively. Adhesion strengths of hBN- and SiO_2-resins on various substances are summarized in Fig. 11. We note that for PCB specimen, the fracture propagated along the resin matrix and for other three types of specimens, the fracture occurred at the resin/substrate interfaces. Hence the adhesion data for PCB substrate do not represent the true adhesion strength of resin/PCB interface. For the other three substrates, the adhesion strengths was in the order of Al_2O_3 > Si wafer > PbSn solder. The polarity is defined as the ratio of the polar component, γ^p, to the total surface free energy, γ^s [29]. It is expected that an increasing polarity of substrate surface offers a higher wettability for intimate contact of resin on substrate and hence a stronger interfacial bond [30]. Polarities of Al_2O_3, Si wafer, and PbSn solder are known to be in the order of 0.79 [31] > 0.62 [29] > 0.32 [29], which is in consistent with the results of adhesion measurements. Figure 11 also shown that the adhesion strengths of SiO_2-resin on various substrates investigated in this work are higher than those for hBN-resin. This is attributed to the fact that the hydroxide bonds on SiO_2 surface benefit the formation of interfacial bonding [32].

The adhesion strengths as a function of filler content of hBN-resin on various substrates are given in Fig. 12. Existence of inorganic fillers would reduce the contact area of resin when applied on the substrate. The increase of filler content decreases

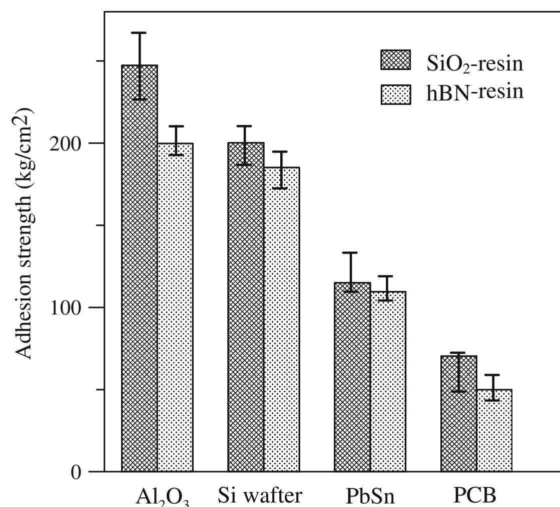

Fig. 11. Adhesion strengths of hBN- and SiO_2-resins on various types of substrates.

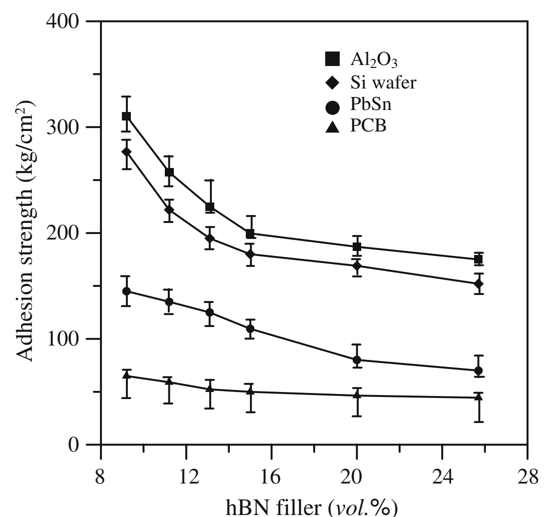

Fig. 12. Adhesion strengths as a function of filler content of hBN-resin on various substrates.

the contact area of resin and hence the adhesion strength decreases accordingly.

3.6. Viscosity of hBN-resin

Viscosity is the key property affecting the dispensation of encapsulation resin. As shown in Table II, viscosity of hBN-resin increases with the increase of filler content. We note that the resin samples became rather immobile when hBN content is higher than 20 vol.%. Pujari *et al.* [33] reported that large surface area resulted from non-spherical hBN has might grab more polymer in the vicinity of the filler surface. The amount of polymer that may freely flow is thus reduced and the viscosity of composite resin consequently increases.

4. CONCLUSIONS

This work investigated the effects of hBN filler on the physical properties of composite resin for device encapsulation. It was found that the dielectric constant of hBN-resin decreases with the increase of test frequency but increases with the increase of filler content. The dielectric constant and tangent loss of composite resins were correlated with the presence of polar groups in the filler. The interfacial polarization of SiO_2 is larger than that of hBN due to the existence of hydroxyl (–OH) group on the surface of SiO_2. The dielectric properties of SiO_2-resin is hence inferior to that of hBN-resin.

Thermal property analysis using DSC indicated that addition of hBN filler into epoxide resin effectively increases the conversion and T_g's of composite resins. This evidenced that the amine groups on the plane edges of hBN filler are able to promote the polymerization and therefore enhance the crosslinking of composite resins subjected to thermal curing.

Thermal conductivities of composite resins were increased with increasing content of hBN filler. Thermal conductivity of hBN-resin with 25.7 vol.% filler content is equal to 1.08 W/m K, which is higher than that of SiO_2-resin at 0.43 W/m K.

Adhesion strength of hBN-resin on various substrate materials was in the order of: $Al_2O_3 > Si$ wafer > eutectic PbSn solder. Increase of filler content would deteriorate the adhesion strength of hBN-resin on these materials.

The shape of filler in organic matrix affects viscosity of resin. Though non-spherical shape of hBN benefited the thermal conductivity of composite resin, it inhibited the flow of composite resin that the resins became relatively immobile when filler content was higher than 20 vol.%.

Table II. Viscosity of hBN-Resin

hBN (vol.%)	Viscosity (cPs)
25.7	28493
20.0	19493
15.0	6667
13.1	4667
11.2	3000
9.2	2333

ACKNOWLEDGMENTS

This work was supported by the Ministry of Education, Taiwan, Republic of China within the Project of Excellence "Semiconducting Polymers and Organic Molecules for Electroluminescence: B. Development of Advanced Materials and Devices for Organic Light Emitting Diodes (OLED) Technology" under Contract No. 91-E-FA04-2-4.

REFERENCES

1. C. P. Wong, M. B. Vincent, and S. Shi, *IEEE Trans. Compon. Packaging Manuf. Technol. A* **21**, 360 (1998).
2. P. Gonon, *J. Mater. Sci. Mater. Med.* **12**, 81 (2001).
3. X. S. Dai, M. V. Brillhart, M. Roesch, and P. S. Ho, *IEEE Trans. Compon. Packaging Technol.* **23**, 117 (2000).
4. A. A. Solomo, J. Fourcade, S. G. Lee, S. K. Kuchibhotla, S. Revankar, R. Latta, P. L. Holman, and J. K. McCoy, Proceedings of the 2004 international Meeting on LWR Fuel Performance, Orlando, Florida, 1028 (2004).
5. M. Hussain, Y. Oku, A. Nakahira, and K. Niihara, *Mater. Lett.* **26**, 177 (1996).
6. P. Bujard, G. Kühlein, S. Ino, and T. Shiobara, *IEEE Trans. Compon. Packaging Manuf. Technol. A* **17**, 527 (1994).
7. Y. Xu, D. D. L. Chung, and C. Mroz, *Compos. Pt. A-Appl. Sci. Manuf.* **32**, 1749 (2001).
8. W. Kim, J. W. Bae, I. D. Choi, and Y. S. Kim, *Polym. Eng. Sci.* **39**, 756 (1999).
9. J. W. Bae, W. Kim, S. W. Park, C. S. Ha, and J. K. Lee, *J. Appl. Polym. Sci.* **83**, 2617 (2002).
10. M. T. Huang and H. Ishida, *J. Polym. Sci. B Polym. Phys.* **37**, 2360 (1999).
11. R. S. Pease, *Acta Crystallogr.* **5**, 236 (1952).
12. J. Park, J. S. Lee, and C. C. Lee, Electronic Components and Technology Conference, 2003, Proceedings, 53rd, 1800 (2003).
13. N. M. Mohsen, R. G. Craig, and F. E. Filisko, *J. Biomed. Mater. Res.* **39**, 252 (1998).
14. H. C. Chien, M. H. Tseng, W. W. Ke, C. Y. Wang, and Y. S. Chen, US Patent 6663278 B1 (2003).
15. D. Lu, D. Wong, and C. P. Wong, *J. Electron. Manuf.* **9**, 241 (1999).

16. J. E. Frommer, R. R. Chance, and A. R. Corporation, in *Electrical and Electronic Properties of Polymers: A State-of-the-Art Compendium*, J. I. Kroscheitz, ed. (Wiley, New York, 1988), pp. 101–181.
17. S. H. Mansour and S. L. ABD-EL-Messieh, *J. Appl. Polym. Sci.* **83**, 1167 (2002).
18. S. George, K. T. Varughese, and S. Thomas, *J. Appl. Polym. Sci.* **73**, 255 (1999).
19. Y. C. Chen, H. C. Lin, and Y. D. Lee, *J. Polym. Res.* **10**, 247 (2003).
20. J. B. Birks and J. H. Schulman, *Progress in Dielectrics* (New York, 1959), Vol. I, pp. 256–261.
21. R. L. Smith Jr., S. B. Lee, H. Komori, and K. Arai, *Fluid Phase Equilib.* **144**, 315 (1998).
22. S. X. Wu, C. Zhang, C. P. Yeh, S. Wille, and K. Wyatt, Proceedings of the 47th Electronic Components and Technological Conference, 550 (1997).
23. H. P. Higginbottom, US Patent 4501864 (1985).
24. H. P. Higginbottom and M. F. Drumm, US Patent 4557979 (1985).
25. C. P. Wong and R. S. Bollampally, *J. Appl. Polym. Sci.* **74**, 3396 (1999).
26. J. Qu and C. P. Wong, *IEEE Trans. Compon. Packaging Technol.* **25**, 53 (2002).
27. G. Wang, J. H. Zhao, M. Ding, and P. S. Ho, Inter Society Conference on Thermal Phenomena, pp. 869–875 (2002).
28. M. Bonneau and J. Stewart, Proceedings of the International Symposium and Exhibition on Advanced Packaging Materials Processes, Properties and Interfaces, 57 (1997).
29. M. L. Sham and J. K. Kim, *J. Adhes. Sci. Technol.* **17**, 1923 (2003).
30. S. J. Luo and C. P. Wong, *IEEE Trans. Compon. Packaging Technol.* **24**, 43 (2001).
31. D. J. Siegel, L. G. Hector, and J. B. Adams, *Phys. Rev. B* **67**, 092105-1 (2003).
32. C. P. Wong and R. S. Bollampally, *IEEE Trans. Adv. Packag.* **22**, 54 (1999).
33. V. K. Pujari, W. T. Collins, and J. J. Kutsch, US Patent 6645612B2 (2003).